IAC-24-C2,1,x88850

Nonlinear thermo-elastic analysis of laminated composite structures for spacecraft

F. Bracaglia[1]*, A. Pagani[2], E. Zappino[3] and E. Carrera[4]

[1] *Mul2 Lab, Department of Mechanical and Aerospace Engineering, Politecnico di Torino, Corso Duca degli Abruzzi 24, 10129 Torino, Italy,* francesca.bracaglia@polito.it
[2] *Mul2 Lab, Department of Mechanical and Aerospace Engineering, Politecnico di Torino, Corso Duca degli Abruzzi 24, 10129 Torino, Italy,* alfonso.pagani@polito.it
[3] *Mul2 Lab, Department of Mechanical and Aerospace Engineering, Politecnico di Torino, Corso Duca degli Abruzzi 24, 10129 Torino, Italy,* enrico.zappino@polito.it
[4] *Mul2 Lab, Department of Mechanical and Aerospace Engineering, Politecnico di Torino, Corso Duca degli Abruzzi 24, 10129 Torino, Italy,* erasmo.carrera@polito.it

Abstract

This research aims to describe the complex behaviour of composite structures under thermal load. The problem is formulated within the Carrera Unified Formulation framework, which allows a compact and hierarchical implementation of high-order structural theories. The thermal problem is schematized using a decoupled approach, where the thermal profile is assumed to be known and treated as an external load. The nonlinear equations are solved by the Finite Element Method using the Newton-Raphson algorithm. Comparative analyses between linearized and nonlinear approaches highlight the importance of nonlinear analysis of the thermal effect for these structures. The importance in evaluating the stress distribution through non-linear analyses for high-precision application structures is also assessed.

Keywords: *non-linear analysis, thermo-elastic analysis, non-linear stress, FEM*

Nomenclature

$\boldsymbol{u}$	Displacement vector
$\boldsymbol{u}_\tau$	2D displacement vector
$\boldsymbol{\epsilon}$	Strain vector
$\boldsymbol{\epsilon}_l$	Vector of the mechanical linear strain
$\boldsymbol{\epsilon}_{nl}$	Vector of the mechanical non-linear strain
$\boldsymbol{\epsilon}_\theta$	Vector of the thermal linear strain
$\boldsymbol{\sigma}$	Stress vector
$\boldsymbol{\sigma}_l$	Vector of the mechanical linear stress
$\boldsymbol{\sigma}_{nl}$	Vector of the mechanical non-linear stress
$\boldsymbol{\sigma}_\theta$	Vector of the thermal linear stress
$\boldsymbol{C}$	Material properties matrix
$\boldsymbol{b}_l$	Linear differential operator
$\boldsymbol{b}_{nl}$	Non-linear differential operator
$\boldsymbol{\alpha}$	Vector of the thermal expansion coefficients
$\boldsymbol{\beta}$	Vector of the thermo-mechanical coupling coefficients
ΔT	Applied over-temperature
N	Number of expansion terms
M	Order of shape functions
τ, i, s, j	CUF assembling indices
$\boldsymbol{F}_\tau$	Expansion functions
N_i	Shape functions
$\boldsymbol{q}$	Nodal displacements
δL_{int}	Variation of the virtual internal work
δL_{ext}	Variation of the virtual external work
$\boldsymbol{K}_s$	Secant stiffness matrix
$\boldsymbol{K}_T$	Tangent stiffness matrix
$\boldsymbol{F}_\theta$	Thermal load vector
$\widetilde{\boldsymbol{F}}_\theta$	Tangent thermal load vector
$\boldsymbol{\varphi}_{res}$	Residual vector
λ	Load scaling factor
$\boldsymbol{K}_{\sigma\theta}$	Thermal geometrical tangent matrix

Acronyms/Abbreviations

EUS	Exploration Upper Stage
PVD	Principle of Virtual Displacements
CUF	Carrera Unified Formulation
FEM	Finite Element Method
CLT	Classical Lamination Theory
FSDT	First Shear Deformation Theory
FN	Fundamental Nuclei
BC	Boundary Condition
LE2	2nd order Lagrange Expansion function
Q9	Bi-quadratic plate FEM element

1. Introduction

Laminated composite structures still attract the interest of the space industry for several reasons, including lightweight, tenable anisotropy allowing for tailored thermo-elastic stability and integration of components through one-peace manufacturing [1]. Applications of fiber-reinforced materials include strap elements, booms, deployable structures and solar arrays, antennas, and payload shrouds [2]. An example of the successful use of laminates is the NASA Space Launch System (SLS), which demonstrated the effective use of these materials in the production of payload faring, EUS, and lightweight joints to join large rocket structures [3].

The cited applications of laminate represent a very challenging field of study for the high precision that is necessary in the numerical description of the structural behaviour. Furthermore, the load conditions to which the structures are subjected, are very extreme and vary in a significant range of temperatures.

Indeed, of the various solicitations that exist in space, thermal variations are among those of greatest interest. As a consequence, over the years, different analyses have been conducted to study the influence of thermal load on the behaviour of structures. Many analyses have been published over the years. Among these, Carrera deeply analyzes the influence of the thermal profile in [4], and the thermal stress is investigated in [5]. Different authors have investigated thermal instability for various materials through a linearized formulation [6, 7].

During the years, the necessity in the use of non-linear description in combination with high-order theories is extensively assessed when the application of a mechanical load is considered [8,9]. Furthermore, also the necessity in the non-linear thermal description has been studied and discussed for both, post-buckling description and large-deformation response during the application of a thermal load.

Mayers et. al. [10] employed variational methods in conjunction with a Rayleigh-Ritz formulation in order to describe the buckling and post-buckling response of different laminated plates subjected to constant thermal load. Huang et al. [11] studied the post-buckling behaviour of plates through the principle of minimum potential energy and incremental loading method.

The present work aims to study the thermo-elastic behaviour of laminated plates, investigate the non-linear post-buckling, and describe the stress trend obtained through the use of CUF.

The CUF is a framework which allows to schematize the structural problem in an efficient and rigorous manner allowing to use high-order theories to better describe multifield problem [12]. Its efficiency is demonstrate in various application such as thermal frequency study [13], linearized thermal buckling [14] and non-linear analysis of hyperplastic materials [15].

The article is organized as follows: in Section 2, some preliminaries about the thermal and mechanical formulation are outlined. In Section 3, the non-linear equations are obtained through the use of the CUF. Finally in Section 4 some numerical results are obtained and in the Conclusions some final considerations are outlined.

2. Preliminaries

The present work investigates a steady-state thermo-mechanical problem using a decoupled approach. This assumption of a known thermal profile along the thickness is realistic because the thermal profile is constant throughout the very thin plate.

As a first approximation, the material properties do not change when the applied temperature increases.

The primary variables of the problem are the pure displacement components reported in Eq. (1).

$$\boldsymbol{u}^T = (u_x, u_y, u_z) \tag{1}$$

Where the apex T means transposition. Strains $\boldsymbol{\epsilon}$ and stresses $\boldsymbol{\sigma}$ are expressed in vectorial form as reported in Eq.s. (2) and (3), respectively.

$$\boldsymbol{\epsilon}^T = (\epsilon_{xx}, \epsilon_{yy}, \epsilon_{zz}, \epsilon_{xz}, \epsilon_{yz}, \epsilon_{xy}) \tag{2}$$
$$\boldsymbol{\sigma}^T = (\sigma_{xx}, \sigma_{yy}, \sigma_{zz}, \sigma_{xz}, \sigma_{yz}, \sigma_{xy}) \tag{3}$$

The non-linear geometrical relations are expressed through the Green-Lagrange strain components considering the differential operators $\boldsymbol{b}_l$ and $\boldsymbol{b}_{nl}$ that collect the linear and non-linear terms, respectively. The relation between strains and displacement is expressed in Eq. (4).

Furthermore, it is worthwhile to decompose strains and stresses in mechanical (linear and non-linear) and thermal components where temperature and strains are related through the vector of thermal expansion coefficients $\boldsymbol{\alpha}$.

$$\boldsymbol{\epsilon} = \boldsymbol{\epsilon}_l + \boldsymbol{\epsilon}_{nl} + \boldsymbol{\epsilon}_\theta = (\boldsymbol{b}_l + \boldsymbol{b}_{nl})\boldsymbol{u} - \boldsymbol{\alpha}\Delta T \tag{4}$$

In this work, composite plates are considered. The link between stresses and strains is reported in Eq. (6), expressed through the well-known material properties matrix denoted as $\boldsymbol{C}$ [16] expressed here in the Cartesian global reference system.

$$\boldsymbol{\sigma} = \boldsymbol{\sigma}_l + \boldsymbol{\sigma}_{nl} + \boldsymbol{\sigma}_\theta \tag{5}$$
$$\boldsymbol{\sigma} = \boldsymbol{C}(\boldsymbol{\epsilon}_l + \boldsymbol{\epsilon}_{nl} - \boldsymbol{\alpha}\Delta T) = \boldsymbol{\sigma}_l + \boldsymbol{\sigma}_{nl} - \boldsymbol{\beta}\Delta T \tag{6}$$

The problem is schematized through the CUF in conjunction with FEM.

The CUF is an efficient framework that describes the different kinematic theories from the classical, such as CLT or FSDT, to the high-order theories without limits in the expansion order or the number of unknowns in the single node. In describing two-dimensional problems, the CUF allows us to express the three-dimensional displacement $\boldsymbol{u}(x, y, z)$ by combining of the two-dimensional displacement vector $\boldsymbol{u}_\tau(x,y)$ and the expansion functions $\boldsymbol{F}_\tau(z)$ as reported in Eq. (7).

$$\boldsymbol{u}(x,y,z) = \boldsymbol{F}_\tau(z)\,\boldsymbol{u}_\tau(x,y) \quad \tau = 1,2,\dots,N \tag{7}$$

This formulation can be easily implemented in conjunction with FEM, as reported in Eq. (8).

$$\begin{gathered}\boldsymbol{u}(x,y,z) = \boldsymbol{F}_\tau(z)\,N_i(x,y)\boldsymbol{q}_{\tau i} \\ \tau = 1,2,\dots,N \qquad i = 1,2,\dots,M\end{gathered} \tag{8}$$

3. Non-linear problem outline

The governing equation is obtained through the PVD, in which the equality between the variations of the virtual internal and external work is imposed, as reported in Eq. (9).

$$\delta L_{int} = \delta L_{ext} \tag{9}$$

When the mechanical load is null, the virtual external work is zero. As a consequence, only the virtual internal work is used to determine the governing equations.

The structural problem is written through CUF and FEM in terms of FN [12] as reported in Eq. (10), and the corresponding assembled form is written in Eq. (11).

$$\boldsymbol{K}_s^{ij\tau s}\boldsymbol{q}^{\tau i} - \boldsymbol{F}_\theta^{sj} = 0 \tag{10}$$

$$\boldsymbol{K}_s\,\boldsymbol{q} - \boldsymbol{F}_\theta = 0 \tag{11}$$

In the case of non-linear studies, matrix $\boldsymbol{K}_s$ is the non-linear secant stiffness matrix that contains the principal unknowns of the problem. As a consequence, Eq. (11) represents a non-linear set of equations that is usually solved using an incremental linearized scheme, the Newton-Raphson method. According to this method, Eq. (11) is written as:

$$\boldsymbol{\varphi}_{res} = \boldsymbol{K}_s\,\boldsymbol{q} - \boldsymbol{F}_\theta = 0 \tag{12}$$

Where $\boldsymbol{F}_\theta$ depends on ΔT, Eq. (12) in Taylor's series about the known solution, became:

$$\begin{gathered}\boldsymbol{\varphi}_{res}(\boldsymbol{q}+\delta\boldsymbol{q},\Delta T+\delta\Delta T) = \\ \boldsymbol{\varphi}_{res}(\boldsymbol{q},\Delta T) + \frac{\partial\boldsymbol{\varphi}_{res}}{\partial\boldsymbol{q}}\delta\boldsymbol{q} + \frac{\partial\boldsymbol{\varphi}_{res}}{\partial(\Delta T)}\delta\lambda(\Delta T)_{ref} \\ = 0\end{gathered} \tag{13}$$

Where $\frac{\partial\boldsymbol{\varphi}_{res}}{\partial\boldsymbol{q}} = \boldsymbol{K}_T$ and $-\frac{\partial\boldsymbol{\varphi}_{res}}{\partial(\Delta T)} = \widetilde{\boldsymbol{F}}_\theta$. Furthermore, it is assumed that the temperature varies directly with the reference temperature.

The equation is written in a compact form in Eq. (14) and necessitates a constraint equation for the load scaling parameter λ.

$$\begin{cases}\boldsymbol{K}_T\delta\boldsymbol{q} = \widetilde{\boldsymbol{F}}_\theta\,\delta\lambda(\Delta T)_{ref} - \boldsymbol{\varphi}_{res}(\boldsymbol{q},\Delta T) \\ c(\delta\boldsymbol{q},\delta\Delta T) = 0\end{cases} \tag{14}$$

The load vector that multiplies the load scaling parameter is a non-conservative load, which depends on the unknown of the problem. As a consequence, the chosen control method to solve the system is the path-following method with arc-length constraint which details can be found in [17,18].

The procedure outlined thus far is analogous to the conventional definition of a mechanical problem. The main differences due to the thermal contribution are outlined in the following section.

4. Explicit formulation of the thermo-mechanical matrices

The secant stiffness matrix and the thermal load vector are defined directly through the principle of virtual displacement.

The explicit formulation of the PVD is reported in Eq. (15):

$$\begin{gathered}\delta L_{int} = \int_V \delta\boldsymbol{\epsilon}^T\boldsymbol{\sigma}dV \\ = \int_V \delta(\boldsymbol{\epsilon}_l+\boldsymbol{\epsilon}_{nl})^T\boldsymbol{C}(\boldsymbol{\epsilon}_l+\boldsymbol{\epsilon}_{nl}+\boldsymbol{\epsilon}_\theta)dV\end{gathered} \tag{15}$$

The only term that differs from the mechanical problem is:

$$\int_V \delta(\boldsymbol{\epsilon}_l+\boldsymbol{\epsilon}_{nl})^T\boldsymbol{\sigma}_\theta dV \tag{16}$$

Substituting the definition of thermal stress reported in Eq. (6) and the geometrical relation outlined in Eq. (4) in Eq. (16), it is possible to obtain the linear and non-linear terms of $\boldsymbol{F}_\theta$ in terms of FN.

$$\int_V \delta\left(\boldsymbol{b}_l F_s N_j \boldsymbol{q}_{sj} + \boldsymbol{b}_{nl} F_s N_j \boldsymbol{q}_{sj}\right)^T \boldsymbol{\beta}\Delta T\, dV \tag{17}$$

Where s and j are analogous to τ and i, respectively, but are referred to the virtual variation. It is possible to obtain the matrix $\boldsymbol{B}$ applying the differential operator $\boldsymbol{b}$ to the shape and expansion function. When the virtual variation is applied to the matrix $\boldsymbol{B}$, as reported in [18], it is possible to demonstrate that:

$$\begin{gathered}\delta(\boldsymbol{B}_l\boldsymbol{q}) = \boldsymbol{B}_l\,\delta\boldsymbol{q} \\ \delta(\boldsymbol{B}_{nl}\boldsymbol{q}) = 2\delta\boldsymbol{q}\,\boldsymbol{B}_{nl}\end{gathered} \tag{18}$$

As a consequence, Eq. (17) becomes:

$$\delta \boldsymbol{q}^{sj^T}\left(\int_V \boldsymbol{B}_l^{sj^T}\, dV + 2\int_V \boldsymbol{B}_{nl}^{sj^T} dV\right) \boldsymbol{\beta}\Delta T = \delta \boldsymbol{q}^{sj^T}[\boldsymbol{F}_{\theta_l}^{sj} + \boldsymbol{F}_{\theta_{nl}}^{sj}] \tag{19}$$

The thermal components affect the vector of thermal load, which can be expressed through the sum of linear and non-linear terms. The secant stiffness matrix remains unchanged when a thermo-mechanical decoupled approach is chosen.

The tangent stiffness matrix is obtained through the second variation of the PVD.

$$\delta(\delta L_{int}) = \delta \int_V \delta\boldsymbol{\epsilon}^T \boldsymbol{\sigma} dV = \int_V \delta^2(\boldsymbol{\epsilon}_l + \boldsymbol{\epsilon}_{nl})^T \boldsymbol{\sigma} dV + \int_V \delta(\boldsymbol{\epsilon}_l + \boldsymbol{\epsilon}_{nl})^T \delta\boldsymbol{\sigma} dV \tag{20}$$

The second term of Eq. (20) is composed only of mechanical terms and is not changed by considering the thermal problem. On the other hand, the first term of Eq. (20) makes it possible to obtain the geometrical stiffness tangent matrix, which can be considered as composed of the summation of $\boldsymbol{K}_\sigma$ and $\boldsymbol{K}_{\sigma\theta}$ where the latter matrix can be defined as in Eq. (21).

$$\boldsymbol{K}_{\sigma\theta} = \int_V \delta^2 \boldsymbol{\epsilon}_{nl}^T \boldsymbol{\sigma}_\theta dV \tag{21}$$

The others terms are not defined here because they can be easily found in the literature [18].

5. Numerical results

Following, some numerical results are reported. The analysis is conducted on a square laminated plate composed of graphite-reinforced composite with simply supported constraint. The results of the post-buckling behaviour are compared to the one published by Meyers et al. [10].

The constraints are applied on the middle plane of the plate and are described in Eq. (22):

$$\begin{array}{ll} at\ \ x = -{}^{L}/_{2}, {}^{L}/_{2} & at\ \ y = -{}^{L}/_{2}, {}^{L}/_{2} \\ u_x = 0, & u_y = 0, \\ u_z = 0 & u_z = 0 \end{array} \tag{22}$$

Thermal load is constant along the thickness and in the plate plane.

The geometry of the plate is reported in Fig. 1 with the used reference system. The plate edges L are 152.4 mm, and each layer is 0.127 mm with a total plate thickness of h=1.016 mm. The lamination is symmetric, composed of eight layers with a quasi-isotropic stacking sequence [45/-45/0/90]s.

The material properties are here reported, $E_1 = 155.00$ GPa, $E_2 = E_3 = 8.07$ GPa, $\nu = 0.22$, $G_{12} = G_{13} = 4.55$ GPa, $\alpha_1 = -0.07x\,10^{-6}\,1/C$, $\alpha_2 = \alpha_3 = 30.1x\,10^{-6}\,1/°C$.

The material properties are considered constant for the whole analysis and unchanged with respect to the applied temperature.

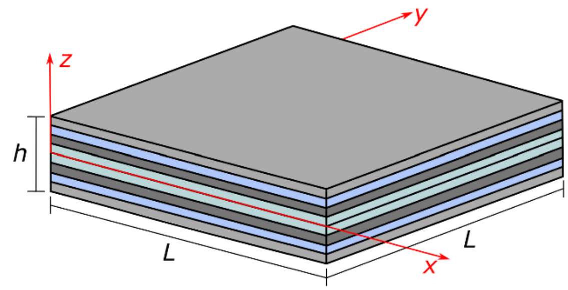

Figure 1: Plate geometry and reference system.

Tables 1 and 2 collect the results of the convergence analyses. The results are obtained by increasing the number of in-plane Q9 elements, with an in-thickness expansion function of one LE2 for each layer.

Table 1 reports a first convergence analysis comparing the linearized critical buckling temperature. The procedure used to obtain these results, while not reported here, is fully detailed and available in [14], providing a comprehensive understanding of our research process.

Table 1: Linear convergence analysis, one LE2 each layer.

N of Q9	5x5	8x8	10x10	13x13
ΔT_{cr}[°C]	38.65	38.30	38.26	38.18
DOF	6171	14739	22491	37179

From the results in Table 1, the 10 x 10 Q9 mesh discretization can be chosen to obtain accurate results. On the other hand, the main focus of this work is the non-linear analysis and a convergence analysis solving the non-linear equations is necessary to choose a better discretization. The convergence analysis is conducted also through non-linear analyses and the results are shown in terms of non-dimensional overtemperature and non-dimensional z-displacement.

Table 2: non-linear convergence analysis, one LE2 each layer.

N of Q9	5x5	8x8	10x10	13x13

$\Delta T/\Delta T_{cr}$	u_z/h			
0.895	3.24×10^{-4}	3.21×10^{-4}	3.20×10^{-4}	3.19×10^{-4}
1.16	0.370	0.371	0.374	0.375
2.85	1.24	1.25	1.26	1.26

Due to the results reported in Tables 1 and 2, a discretization of 10 x 10 Q9 is chosen. The following results are obtained through a 10 x 10 Q9 in-plane discretization.

Figure 2 displays the overtemperature-displacement graph. The z-displacement is taken in the center of the plate at point P(0,0,0), and the overtemperature is in non-dimensional form with respect to the bifurcation point temperature calculated through the linearized analysis.

For the considered plate, the linearized buckling critical temperature is reported in Table 1 and is about $\Delta T_{cr} = 38.26\ °C$.

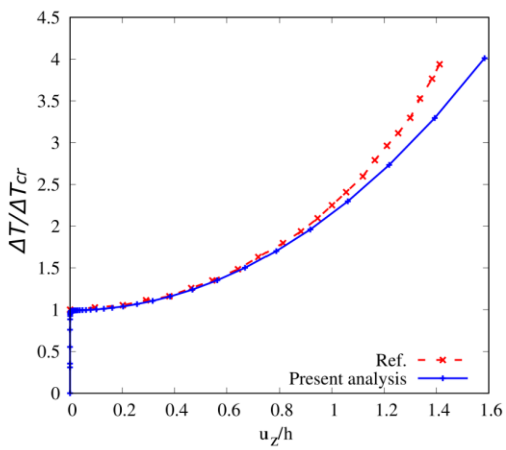

Figure 2: z-displacement and overtemperature graph with non-dimensional value. Reference results from [10].

Figure 2 clearly shows that the results obtained through the present method perfectly overlap with the reference results in the temperature range dominated by linear and moderately non-linear phenomena.

Otherwise, in the case of a high non-linear range, the results are quietly diverging. This divergence is primarily due to the influence of the different descriptions of the non-linearities, which are schematized through the complete Green-Lagrange stress tensor in the present analyses, as opposed to the Von-Kharman non-linearities evaluated in the published results. The influence of this difference in the non-linear studies is detailed in [19].

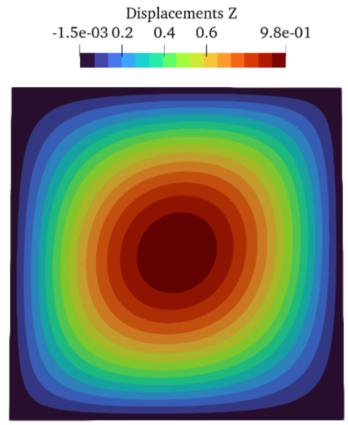

Figure 3: z-displacement for thermal non-dimensional load of 2. 10 x 10 Q9 and LE2 expansion functions.

The displacement distribution along the plate, with a load of $\Delta T/\Delta T_{cr} = 2$, is reported in Fig. 3.

In Fig. 3, the results are expressed in mm. As expected, the maximum displacement is in the center of the plate.

In the study of a laminate subjected to a thermal load, it is important to describe the stress state of the plate. For this reason, in Figures 4 and 5, the in-plane normal and shear stresses are reported.

In order to better clarify the necessity of using a non-linear analysis when a certain temperature value is exceeded, the stresses obtained through linear static analysis are reported together with those obtained through the non-linear analysis described here.

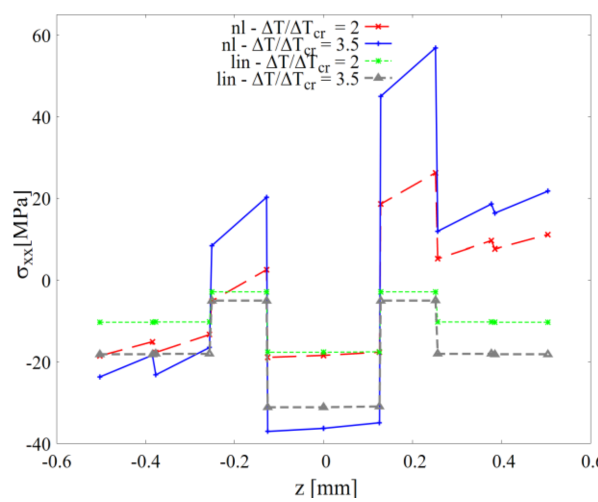

Figure 4: In plane normal stress with different loads. 10 x 10 Q9 and LE2 in-thickness expansion. Comparison between linear and non-linear analyses.

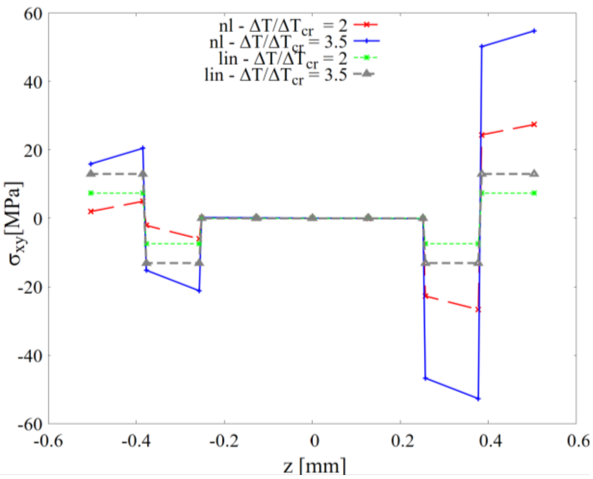

Figure 5: In plane shear stress with different loads. 10 x 10 Q9 and LE2 in-thickness expansion. Comparison between linear and non-linear analyses.

Increasing the thermal load makes the necessity of a non-linear analysis more evident. The results obtained from solving the linear static equations are about the same as the non-linear analysis, only in the center layers of the plate for both the reported stresses. On the other hand, for the stresses with the major entities, which are the ones developed along the external layers of the plate, the error of the linear analysis increases. Furthermore, comparing the non-linear results, the non-linear trend is evident, but the stress distribution remains the same for the two different applied thermal loads.

6. Conclusions

The present work collects some information about the formulation and numerical results for the non-linear thermal analysis. The model is formulated through the use of CUF and FEM, and the governing equations are obtained through the use of PVD. The thermal load is assumed to be constant along the whole plate with a steady state condition, and the decoupled approach is chosen.

The solution of the non-linear equations is obtained using the arc-length constraint. Thanks to the CUF, it is possible to describe not only the load-displacement trend but also the stress distribution.

The reported results prove the necessity of using a non-linear formulation to describe the post-buckling analysis. Furthermore, the results demonstrate that the layer-wise modeling and the non-linear formulation reported here are effective and that the stress can be appropriately described.

Credit authorship contribution statement

F. Bracaglia: Software, Methodology, Validation, Formal analysis, Investigation, Writing - original draft. **A. Pagani**: Methodology, Validation, Conceptualization, Writing – review & editing, Supervision. **E. Zappino**: Conceptualization, Methodology, Software, Supervision. **E. Carrera**: Conceptualization, Supervision.

References

[1] Mangalgiri PD. Composite materials for aerospace applications. Bull Mater Sci 1999;22(3):657–64.
[2] Zaigham ST. Space Applications of Composite Materials. Journal of Space Technology 2018;(8) 65-70.
[3] Eldred LB. NASA Langley Research Center, Hampton, VA, US. International Conference on Emerging Trends in Technology and Applied Sciences. Pathamuttom, April 30, 2015.
[4] Carrera E. Temperature profile influence on layered plates response considering classical and advanced theories. AIAA J 2002;40:1885–96.
[5] Carrera E. An assessment of mixed and classical theories for the thermal stress analysis of orthotropic multilayered plates. J Therm Stress 2000;23(9):797–831.
[6] Thangaratnam KR, Palaninathan, Ramachandran J. Thermal buckling of composite laminated plates. Comput Struct 1989;32(5):1117–24.
[7] Chen WJ, Lin PD, Chen LW. Thermal buckling behavior of thick composite laminated plates under nonuniform temperature distribution. Comput Struct 1991;41(4):637–45.
[8] Pagani A. Carrera E. Large-deflection and post-buckling analyses of laminated composite beams by Carrera Unified Formulation. Comput Struct 2017; 170: 40-52.
[9] Librescu L. Stein M. A geometrically nonlinear theory of transversely isotropic laminated composite plates and its use in the post-buckling analysis. Thin-Walled Structures 1991; 11:177-201.
[10] Mayers CA. Hyer MW. Thermal Buckling and Postbuckling of symmetrically laminated composite plates. J Therm Stress 1991 14:4, 519-540.
[11] Huang NN. Tauchert TR. Postbuckling Response of Antisymmetric Angle-Ply Laminates to Uniform Temperature Loading. Acta Mech 1988 72, 173-183.
[12] Carrera E, Cinefra M, Petrolo M, Zappino E. Finite element analysis of structures through unified formulation. Chichester, West Sussex, UK: John Wiley & Sons; 2014.
[13] Fazzolari FA. Natural frequencies and critical temperatures of functionally graded sandwich plates subjected to uniform and non-uniform temperature distributions. Compos Struct 2015;121:197–210.
[14] Bracaglia F. Masia R. Pagani A. Zappino E. and Carrera E. Thermal buckling of variable stiffness

composite laminates using high order plate finite elements. Compos Struct 2024;345.

[15] Chiaia P. Pagani A. Cinefra M. and Carrera E. Analysis of transversely isotropic compressible and nearly-incompressible soft material structures by high order unified finite elements. Mech Adv Mater Struct 2023; 1-17.

[16] Bathe KJ. Finite element procedures. Bathe, Boston, USA: Bathe, Klaus-Jürgen: Finite element procedures in engineering analysis; 2006.

[17] Crisfield MA. Non-linear Finite Element Analysis of Solid and Structures. John Wiley & Sons, Chichester, England, 1991.

[18] Pagani A. Carrera E. Unified formulation of geometrically nonlinear refined beam theories. Mech Adv Mater Struct. 2016; (25) 15-31.

[19] Pagani A. Carrera E. Augello R. Evaluation of various geometrically nonlinear terms in the static response of beams and thin-walled shell-like structures.